Supporting Information for "Mesoscale Eddies Modulate Mixed Layer Depth Globally"

Peter Gaube[1],Dennis J. McGillicuddy Jr.[2], Aurélie J. Moulin[1]

Contents of this file

1. Text S1 to S3
2. Figures S1 to S4

Additional Supporting Information (Files uploaded separately)

1. Captions for Datasets S1

Introduction This supporting information file details the analysis of two separate mixed layer depth (MLD) products in eddy-centric coordinates with the aim of providing support for the statements made in the main text that the choice of MLD product used in the analysis does not affect

[1]Applied Physics Laboratory, University of Washington, USA

[2]Woods Hole Oceanographic Institution, USA

the conclusions of the study. In addition, we provide another version of the global maps shown in Fig. 1 of the manuscript highlighting regions where the MLD' are significant based on the criteria of exceed the standard error of the observations. In addition, we show that the results presented here are fairly insensitive to the choice of eddy tracking procedure used to identify and track measoscale features. Finally, we provide a NetCDF data file of the MLD anomaly (MLD') maps shown in Fig. 1 of the main text.

Text S1. To quantify the sensitivity of our results to selection of MLD criteria, we computed the MLD anomalies and their climatology from both a density threshold algorthim (DA, Holte and Talley 2009) and from a density threshold method (DT, de Boyer Montegut 2004) where a density increase of 0.03 $kg\ m^{-3}$ from a reference depth at 10 m is used to define the MLD. Holte et al. (2017) report an overall shallower MLD by 10 % using the DA method, which they find to be more accurate compared to the DT method. The difference in MLD climatologies was accentuated in regions of deep winter MLDs. For examples, radial composites computed within eddies indicate that the general trends in both MLD and MLD' are reasonably similar and well within the respective error bars (Fig. S1). Radially averaged MLD' estimated from the DT method tend to be larger in cyclones within a radial distance of L_s (Fig. S1). Radially averaged MLD' estimated from the DT method tends to be larger in cyclones within a radial distance of L_s (Fig. S1). The greatest difference is on the order of 20 m in the Southern Ocean where Holte et al. (2017) also observed increased MLD biases caused by a deeper mixed layer from deep convection during austral winters. The monthly climatologies computed separately for each of the regions described in the manuscript show the same trend between DA and DT as expected with the deeper DT biased discussed above (Fig. S2).

In conclusion, our results of MLD anomalies are robust and do not depend on the criteria for defining MLD or its climatology.

Text S2. The global maps of winter MLD' presented in the manuscript do not include a mask to differentiate values that do not exceed the standard error of the mean. This masking was not applied to the maps shown in Fig. 1 as it result in figures that were too busy and distracted from the central thesis of the work; mesoscale eddies modulate MLD globally. Shown in Fig. S3 are the same maps as presented in Fig. 1 of the manuscript with the exception that geographical bins where the MLD' did not exceed the standard error of the mean are masked with cross hatching. From the maps shown in Fig. S3 we can conclude that in the regions examined in detail in this manuscript, most of the winter MLD' are significantly different than zero (Fig. S3).

Text S3. Our experience using eddy trajectories and characteristics derived using multiple versions of the Chelton method and the Faghmous et al., 2015 method has lead us to conclude that the average imprint of eddies in satellite SST and CHL fields do not change substantially as a result of choice of dataset. We however did not explore how the different eddy datasets influence the results from our analysis of eddy effects on MLD. To determine if further examination of the impact that different eddy trajectories have on this analysis presented here is warranted, we computed eddy-centric monthly climatologies and radial averages of MLD and MLD' in the North Pacific region. We first tracked eddies in a subset of the sea surface height (SSH) observations spanning 2005-2015 in the North Pacific Region using the Faghmous *et al.* (2015) method. Comparing the results using both the Fahmous and Chelton eddies revealed noticeable differences in both the radial averages and climatologies, however, the differences are small and do not suggest that the analysis is particularly sensitive to choice of eddy dataset. For example, maximum MLD occur during February when using the Chelton *et al.* (2011) tracks but this extends from February through March when basing the analysis on the Faghmous *et al.* (2015) eddies (Fig. R1). Additionally, the magnitude of the MLD' during March through June are slightly larger when using the Faghmous eddies (visible as the difference between the red/blue lines and the black line in Fig. R1). The differences resulting from choice of eddy data set are small compared to the variability discussed in the manuscript. It is, however, important to note that larger differences might be expected using eddies derived from methods that use products derived from sea surface height.

Data Set S1. A single NetCDF file containing the following fields:

- latitude
- longitude

- Mean MLD, number of observations in each bin, standard deviation of each bin for anticyclones in winter
- Mean MLD, number of observations in each bin, standard deviation of each bin for anticyclones in summer
- Mean MLD, number of observations in each bin, standard deviation of each bin for cyclones in winter
- Mean MLD, number of observations in each bin, standard deviation of each bin for cyclones in summer

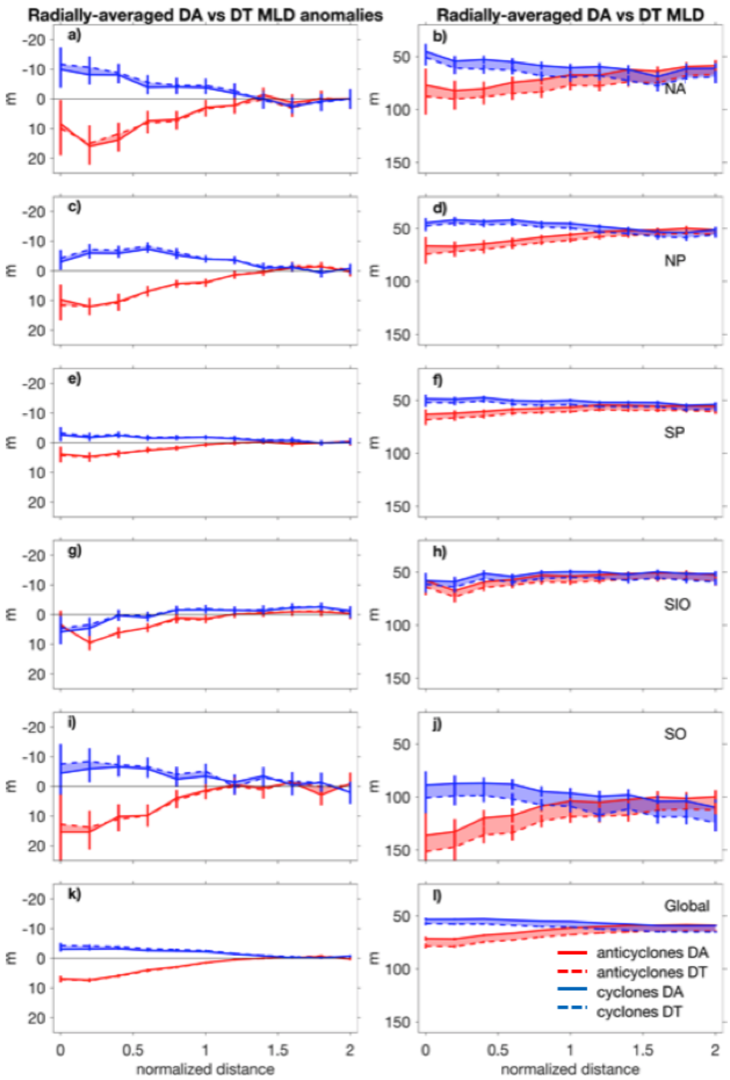

Figure S1. Winter radial averages of MLD' (left column) and MLD (right column) in anticyclones (red) and cyclones (blue) for the 5 regions indicated in Fig. 1 and globally (bottom row). The solid curves show averages made from the density algorithm (DA) MLD estimates and the broken curves from the density threshold (DT) estimates. The shading highlights the differences between the two methods.

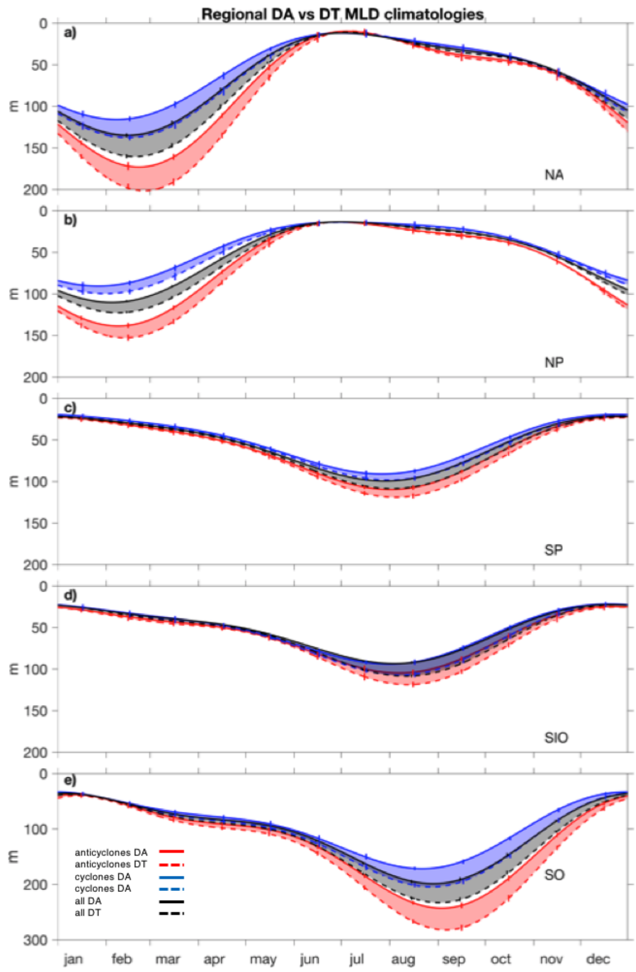

Figure S2. Seasonal cycle of MLD in the North Atlantic Ocean (NA), North Pacific Ocean (NP), South Pacific (SP), South Indian Ocean (SIO), and Indian Ocean sector of the Southern Ocean (SO) regions defined in Fig. 1. The cycles are created by least squares regression of the annual cycle and its first harmonic onto observations in anticyclones (red), cyclones (blue), and all data (black curve). The solid curves show averages made from the density algorithm (DA) MLD estimates and the broken curves from the density threshold (DT) estimates. The shading highlights the differences between the two methods.

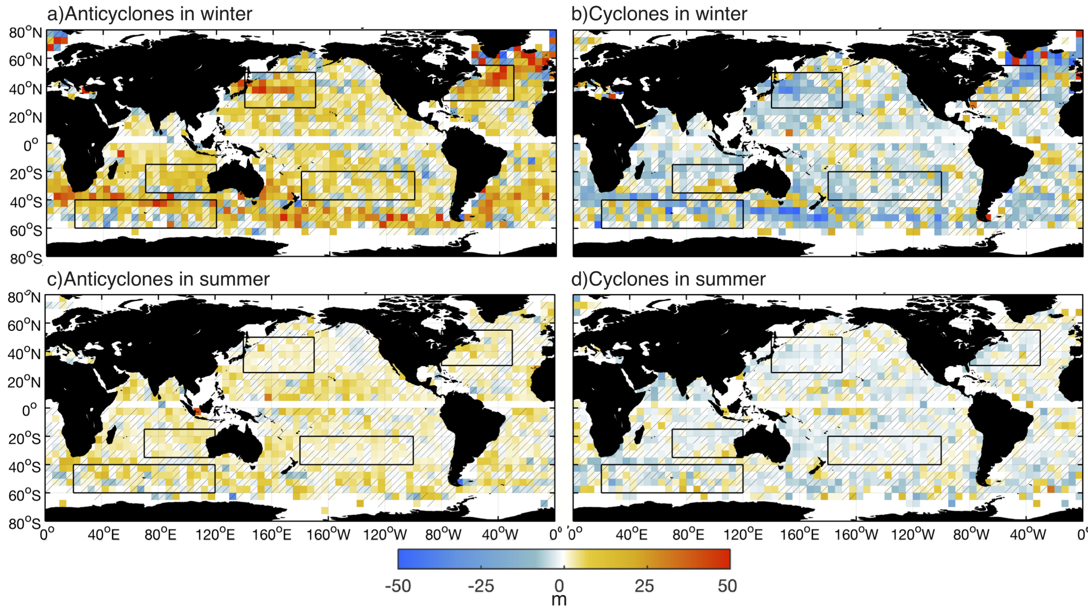

Figure S3. Eddy-induced MLD anomalies (MLD') mapped to a global 5° grid. Observed MLD' within L_s of the center of anticyclones in (a) winter and (c) summer in each hemisphere and cyclones in winter (b) and summer (d) in each hemisphere. Northern hemisphere winter is defined as the period December through March and summer June through September. Southern hemisphere winter is defined as the period June through September and summer December through March. Cross hatching indicates geographical bins that do not exceed the standard error of the mean.

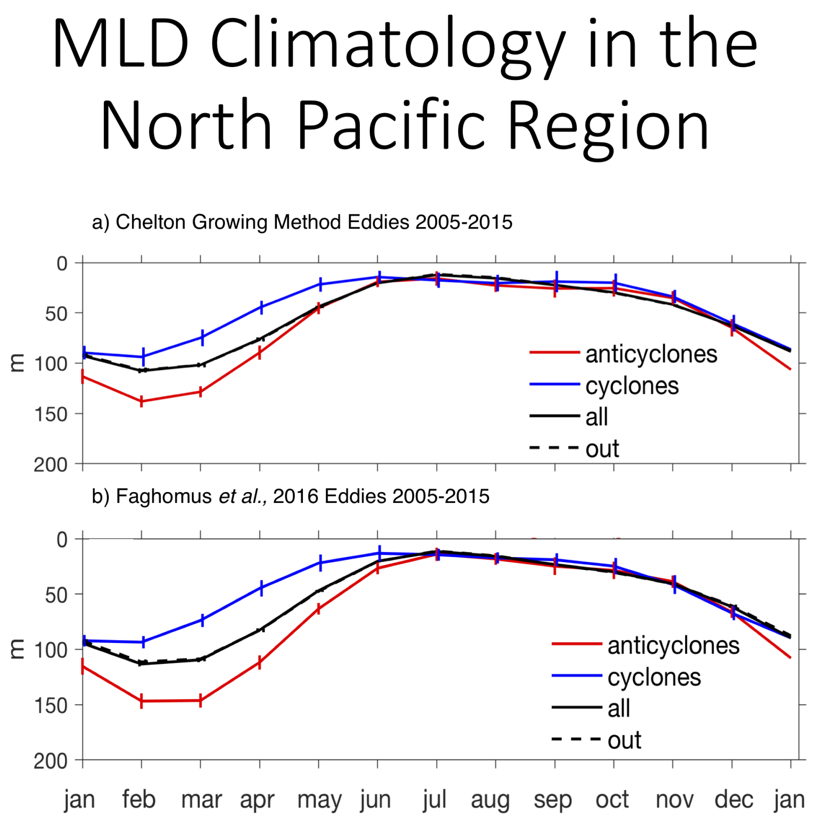

Figure S4. Seasonal cycle of mixed layer depth (MLD) in the North Pacific Ocean (NP) $25°N - 50°N$, $140°E - 190°E$ computed using the (a) Chelton eddies and (b) Faghmous eddies. The cycles are created by least squares regression of the annual cycle and its first harmonic onto observations in anticyclones (red), cyclones (blue), outside of eddies (broken black curve) and all data (black curve). The standard error, computed as $\sigma/\sqrt{N}$ where σ is the standard deviation of all MLD observations during each calendar month and N is the number of MLD observations in each month, is indicated by vertical lines.